Heritage Science

RESEARCH

Open Access

Analysis of *Aspergillus niger* isolated from ancient palm leaf manuscripts and its deterioration mechanisms

Shimin Chu[1,2], Lanying Lin[2] and Xingling Tian[1*]

Abstract

Palm leaf manuscripts (PLMs), venerable historical artefacts containing Buddhist scriptures, history, mathematics and literature, which are carried by palm leaves (*Corypha umbraculifera*) and are highly susceptible to microbial degradation during prolonged storage. This degradation results in significant alterations to both the appearance and material properties of PLMs, but the precise mechanism underlying this deterioration remains a mystery. To this end, the present study focused on ancient PLMs from Xishuangbanna Dai Autonomous Prefecture in Yunnan Province, China. The objective of present study was to isolate, culture and identify the microorganisms typically found in these manuscripts and to use them to biodegrade the carriers of PLMs. Detailed observations of the biodegradation behavior of these microorganisms on the carriers of PLMs were carried out, together with characterizations of the hierarchical structure and mechanical properties of the leaf fiber cell walls. This comprehensive analysis provided insights into the deterioration mechanisms of the carriers of PLMs. The study revealed the presence of the common fungus *Aspergillus niger* on ancient PLMs. *Aspergillus niger* can secrete cellulase, lipase, and acidic substances after colonizing on the carriers of PLMs. These substances sequentially damage the carrier's epidermal cells, mesophyll cells, and leaf fibers, leading to the separation of different tissue structures. At the molecular level, the lipids on the surface of the leaves were degraded initially, and sequential depolymerization of hemicellulose, amorphous cellulose, and crystalline cellulose occurred. Additionally, this study firstly applied nanoindentation technology in the research of PLMs. The mechanical properties of the cell walls underwent notable alterations due to the modifications in chemical and crystalline structure of the carriers of PLMs upon the biodegradation of *Aspergillus niger*. Specifically, the hardness and elastic modulus of leaf fiber cell walls showed an initial increasing and then decreasing trend, consistent with the trend of cellulose crystallinity, which also provided a new reference for assessing the degree of deterioration of PLMs.

Keywords Palm leaf manuscripts, *Aspergillus niger*, Deterioration, Cellulose, Micromechanics

Introduction

Palm leaf manuscripts (PLMs), ancient texts inscribed on palm leaves (*Corypha umbraculifera*), cover diverse fields including history, mathematics, literature, astronomy, art, and medicine [1, 2]. Their unique historical, cultural, artistic, and archaeological value makes them a significant part of the world's cultural heritage. These manuscripts are currently distributed across several countries and regions, including India, Nepal, Sri Lanka, Myanmar, Thailand, Indonesia, Cambodia, and China [2]. They

*Correspondence:
Xingling Tian
13520238749@163.com
[1] China Academy of Cultural Heritage, Beijing 100029, China
[2] Research Institute of Wood Industry, Chinese Academy of Forestry, Beijing 100091, China

serve as a vital resource for understanding Eastern culture. However, after centuries of use, dissemination, and preservation, the PLMs have suffered varying degrees of ageing and damage. This included the embrittlement of the PLM carriers and the fading and flaking of the inscribed ink and pigments [3, 4].

PLM carriers are susceptible to a range of issues due to their biological characteristics and external environmental factors, including insect infestation, mold corrosion, pollution, discoloration, acidification, decay, and mechanical damage [3]. Furthermore, the painted illustrations and inscriptions on these manuscripts suffer blurring or detachment [5]. Current scholarly efforts primarily concentrate on collecting, cataloguing, photocopying, and craft inheritance, with a paucity of research dedicated to the degradation and restoration of PLMs [6, 7]. Zhang et al. [8, 9] investigated the surface pathologies, acidification, and degradation of ancient PLMs from the Potala Palace in Tibet, China, and compared the deterioration of the PLMs under different preservation conditions. However, due to the precious nature of these cultural relics, the research was mostly limited to macro-scale observations. Chu et al. [10] conducted a comparative analysis of the anatomical structure, chemical composition, and mechanical properties of simulated PLMs and ancient PLMs from Burma using diverse characterization techniques to enhance comprehension of the degradation mechanisms of these materials. However, macro-mechanical testing requires large sample quantities and sizes, which has resulted in the destruction of numerous artifacts. Moreover, the reliability of test results is often compromised due to the inhomogeneity of artifact degradation, which limits its application in artifact conservation and assessment [11]. It is important to note that the degradation factors of ancient PLMs are complex and multiple, such as light, temperature, humidity, and biology, making it difficult to identify the degradation mechanism of a single factor [12].

Most organic cultural relics, especially those rich in polysaccharides, are highly susceptible to microbial erosion and degradation, such as paper and wood [13, 14]. PLMs, which use leaves as writing carriers, contain abundant nutrients such as proteins, starches, lipids and cellulose, making them particularly susceptible to mildew [15]. Mildew not only affects the appearance of PLMs, causing the painted images and inscriptions to become blurred or obscured, but also leads to a decline in the mechanical properties of the carriers, significantly limiting their dissemination and utility. Currently, there is lack of reports on the mechanism of mildew-induced degradation of PLMs. The insufficient information hinders the development of effective conservation strategies and poses a challenge to the long-term preservation and legacy of this invaluable cultural heritage. Therefore, understanding the mechanism by which mildew degrades PLMs is essential for conserving this valuable cultural heritage.

In this study, typical microorganism (*Aspergillus niger*) on ancient PLMs from Xishuangbanna Dai Autonomous Prefecture in Yunnan Province, China, were isolated, extracted, cultured and identified. Microbial degradation was then conducted on the PLM carriers using the isolated microorganisms. The hierarchical structures of the PLM carriers after microbial degradation were characterized using various technical methods [16, 17], such as scanning electron microscopy (SEM), X-ray photoelectron spectroscopy (XPS), attenuated total reflectance-Fourier transform infrared spectrometry (ATR–FTIR), and X-ray diffraction (XRD). Additionally, nanoindentation (NI) technology was applied to the PLM carriers for the first time to explore the response mechanism of leaf fiber micromechanics under the microbial degradation. The study aimed to gain a deeper understanding of the process of microbial degradation on PLM carriers and provide scientific basis for future studies about protection of the PLMs and other organic artifacts.

Materials and methods

Materials

Ancient PLMs were obtained from Xishuangbanna Dai Autonomous Prefecture in Yunnan Province, China. The region boasts an annual average relative humidity ranging from 82 to 85%. Coupled with a consistently warm climate throughout the year, these conditions create an exceptionally conducive environment for the growth and proliferation of microorganisms. Thus, the ancient PLMs were wrapped in cotton cloth, then housed within wooden boxes, and finally secured in an airtight room. The environmental conditions within the storage room were controlled at a temperature of 21.9 °C and a relative humidity of 42.0%. However, the proliferation of microorganisms remains inevitable. The microorganism used in the biodegradation experiment were isolated from the ancient PLMs. Fresh palm leaves, sourced from the Xishuangbanna Dai Autonomous Prefecture, were subjected to a series of treatments including trimming, steaming, polishing, flattening, and air-drying, prior to being utilized in microbial degradation experiments. All fresh palm leaves were processed in the same batch, as carrier materials. Potato Dextrose Agar (PDA) medium was purchased from Shanghai Macklin Biochemical Technology Co., Ltd.

Identification of a typical microorganism on the ancient PLMs

A sterile cotton swab dipped in a small amount of 0.85% NaCl was used to swab a typical microorganism visible to the naked eye on ancient PLMs. The obtained sample was then placed in PDA medium for cultivation. Following the emergence of colonies on the PDA medium, individual hyphae were meticulously picked from the colony edges and cultured again on fresh PDA medium to ensure strain purification. This purification process was repeated iteratively until pure strains were obtained, ensuring the absence of any contaminating microorganisms. The purified fungal strains were inoculated onto PDA medium and incubated at a temperature of 28 ± 2 °C with a relative humidity of 85 ± 5% [18]. The growth characteristics of fungal microorganisms on PDA medium were observed, and microscopic morphological features were examined using an optical microscope (CX31, Olympus, Japan). Based on these observations, the typical fungal types were initially identified. Adequate quantities of hyphae and spore aggregates were collected from the purified fungal strains, and their deoxyribonucleic acid (DNA) was extracted. Polymerase chain reaction (PCR) amplification was then carried out using specific primers, and the resulting PCR products were sequenced to accurately identify the fungal species involved.

Microbial degradation

Referring to the Chinese standard GB/T 18261–2013 "Test method for anti-mildew agents in controlling wood mould and stain fungi", the typical fungal suspension was uniformly spread onto PDA medium, and sterilized U-shaped solid glass rods were placed inside. On top of the glass rods, the PLM carrier materials with dimensions of 2 × 4 cm were placed, and finally sealed with a sealing film, and placed in the constant temperature and humidity chamber at a temperature of 28 ± 2 °C and relative humidity of 85 ± 5% for microbial degradation experiment. The experiment lasted for 28 days, with samples being collected every 7 days. Each group consisted of six parallel samples.

Characterization of deteriorated PLM carriers

SEM

The samples designated for the observation of the adaxial or abaxial epidermis were trimmed to dimensions of 5 × 5 mm. The samples designated for the observation of the cross-section were cut into strips with dimensions of 1 × 5 mm and embedded into cubes with dimensions of 15 × 7 × 7 mm using hot melt glue. The primary constituent of this is a base resin derived from the high-pressure copolymerization of ethylene and vinyl acetate. The cross-section of the embedded samples was trimmed into a pyramid shape with a top surface shaped into a square approximately 1 × 1 mm using a single-edged blade. The top surface of the samples was polished using a diamond-knife-equipped ultramicrotome. The samples were secured to a mounting surface with a conductive adhesive tape. They underwent a sputtering process to apply a platinum coating for enhanced electrical conductivity, utilizing an ion sputter coater (E1010, Hitachi, Japan). The SEM imaging was conducted using a high-resolution scanning electron microscope (S-4800, Hitachi, Japan) to acquire detailed images.

XPS

The chemical composition at the surface of the sample was analyze using the XPS (250 Xi, Thermo Fisher, USA). The surface of the samples was wiped clean before the experiment. Each sample was precisely trimmed to a size of 5 × 5 mm and then dried in an oven at 60 °C. The samples were attached to a sample holder and placed inside the XPS's sample chamber. Once the chamber had reached the required vacuum level, the samples were transferred into the analysis chamber. A full-spectrum scan was performed with the following parameters: a spot diameter of 400 μm, an operational voltage of 12 kV, a filament current of 6 mA, a pass energy of 150 eV, and a step size of 1 eV. High-resolution scans were then performed on the C1s spectral range of 279 ~ 298 eV and the O1s spectral range of 525 ~ 545 eV, with a pass energy of 50 eV and a step size of 0.1 eV. The spectra were calibrated using a binding energy of 284.8 eV.

Chemical components content testing

The samples were ground into a powder with a mesh size ranging from 40 to 60, and each sample was replicated three times. The content of ethanol–benzene extractives in samples was measured according to a previous research method [19]. The determination of cellulose, hemicellulose, and lignin content was conducted according to the National Renewable Energy Laboratory (NREL) method [20].

ATR-FTIR

The surface of the degraded PLM carriers was gently wiped clean using a cotton swab. The samples underwent mechanical grinding and sieving, and approximately 200-mesh wood powder was dried in an oven at 60 °C. The powdered samples were then placed in an infrared spectrometer (Nicolet iS5, Thermo Fisher scientific, USA) equipped with a diamond attenuated total reflection crystal attachment for detection. The scanning parameters consisted of 32 scans with a resolution of 4 cm^{-1}. The

absorption range recorded during the analysis spanned from 500 to 4000 cm^{-1}.

XRD

The surface of the samples was cleaned off. The samples underwent mechanical grinding and sieving, and approximately 200-mesh wood powder was dried in an oven at 60 °C. The relative crystallinity of the samples was measured using an XRD (D8 Advanced, Bruker, Germany). The X-ray tube is equipped with a CuKα target. The instrument was operated with a voltage of 40 kV and a current of 40 mA. The scanning range was set to $2\theta = 5 \sim 40°$, with a scan step size of 0.05° and a scan rate of 0.1°/s. The Gaussian function was utilized to fit the reflection peaks for accurate calculation. According to the Segal method [21], the relative crystallinity of the sample was calculated as follows:

$$CI = \frac{I_{200} - I_{am}}{I_{am}} \times 100\% \quad (1)$$

where CI is the crystalline index, I_{200} is the maximum intensity of the (200) crystallographic plane, I_{am} is the intensity of amorphous scattering near the 2θ angle of 18°.

NI

The sample preparation method was consistent with that used for observing cross-sections in SEM experiments. The samples were placed in the TI-950 nanoindentation system (Hysitron, USA) with a relative humidity of approximately 45% and allowed to equilibrate for over three days. The TI-3900 triangular pyramid indenter with an angle of 142.3° and a tip diameter of 100 nm was used. Under load control mode, a three-stage loading function (with loading and unloading times of 5 s and a holding time of 2 s) was applied with a maximum load of 80 μN for nanoindentation testing. During the experiment, load–displacement data was recorded. Subsequently, the hardness and elastic modulus values were calculated using the Oliver-Pharr method [22]. The indentation modulus and hardness of each sample were averaged from at least 30 valid data points.

Data analysis

Data analysis was performed using the statistical software SPSS (IBM SPSS Statistic, version 26, IBM Corporation, New York, USA).

Results and discussion

Microorganism identification

The surfaces of ancient PLMs showed distinct mycelium (Fig. 1a). When typical microorganisms from these ancient manuscripts were isolated and cultured, it was observed that the colonies grew rapidly, took on a flat shape. Initially they appeared as white, velvety structures, eventually changing to brown or dark brown, coarse, velvety colonies with blunt, rounded edges (Fig. 1b). Microscopically, the colonies exhibited circular,

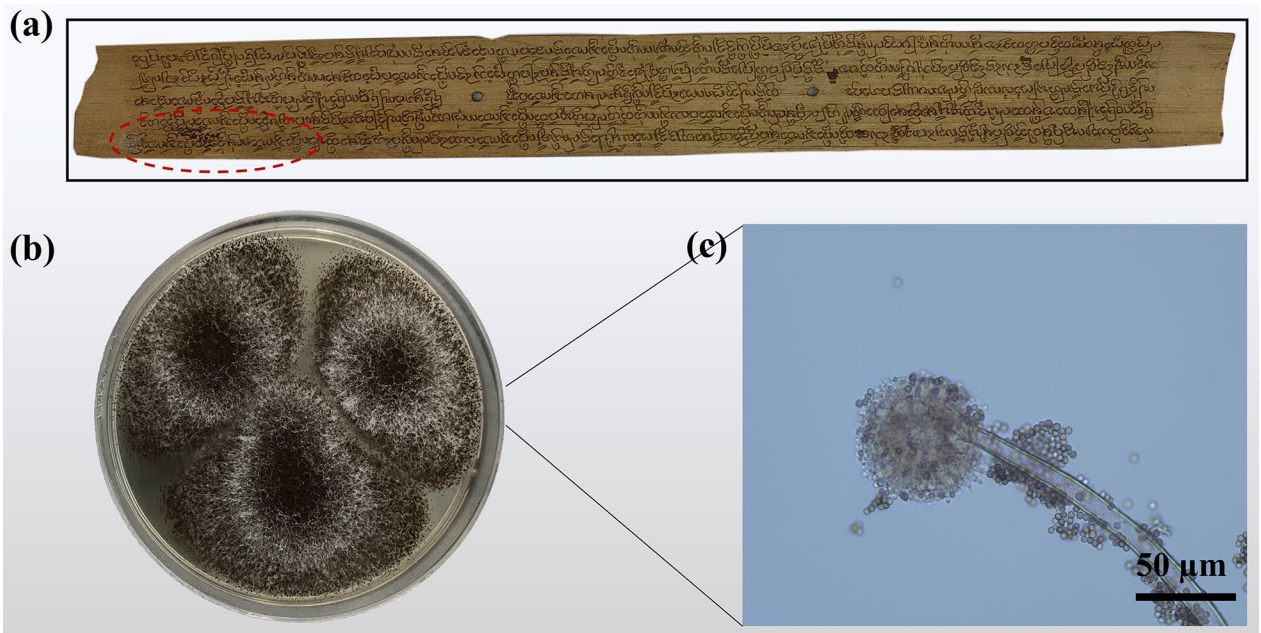

Fig. 1 Macro- and micro-morphological characterization of fungi isolated from ancient PLMs. (**a**) Ancient PLMs, (**b**) Fungal colony, (**c**) Conidiophores

radially arranged conidial heads that were dark brown in color and surrounded by numerous black spores of round or oval shape. The conidiophores were characterized by their elongated length, thick walls, and smooth appearance (Fig. 1c). This was basically consistent with the morphology of *Aspergillus niger* (*A. niger*) [23]. The DNA sequencing results (Additional file) were subjected to comparative analysis on the NCBI website (https://blast.ncbi.nlm.nih.gov/Blast.cgi), and it was found that they share a 99% homology with *A. niger*. Utilizing a combination of DNA extraction, PCR amplification and sequencing, along with macroscopic and microscopic morphological analysis, the microorganism was identified as *A. niger*, belonging to the genus *Aspergillus*, which is a common fungal strain found in ancient paper cultural relics [24, 25].

Morphological structure

The hyphae number of *A. niger* on the surfaces of the PLM carriers increased significantly, leading to a prominent darkening in color (Fig. 2a). Even after undergoing degradation, the PLM carriers retained their overall structural integrity on a macroscopic level. Notable changes in the microstructure of the degraded samples were observed using SEM. With the extension of biodegradation time, the adaxial and abaxial epidermal cells gradually collapsed, and internal structures such as the mesophyll cells with thinner cell walls also severely degraded (Fig. 2f, g). However, the structure of the leaf fiber cell walls remained intact. It was noteworthy that the adaxial and abaxial epidermal cell wall structure of the PLM carriers was compact, making it difficult for *A. niger* conidia, approximately 3.2 μm in diameter, to penetrate the interior of the PLM carriers even upon collapse (Fig. 2c, d). This indicated that although *A. niger* cannot invade the interior of the leaf, its secretions may be able to penetrate through the adaxial and abaxial epidermis of the leaves and invade deeper into the interior. Furthermore, the degradation of internal leaf components induced by *A. niger* resulted in the dissociation of different tissue structures (Fig. 2f, g). This phenomenon could be a crucial contributor to the peeling of ancient PLM surfaces during the storage process.

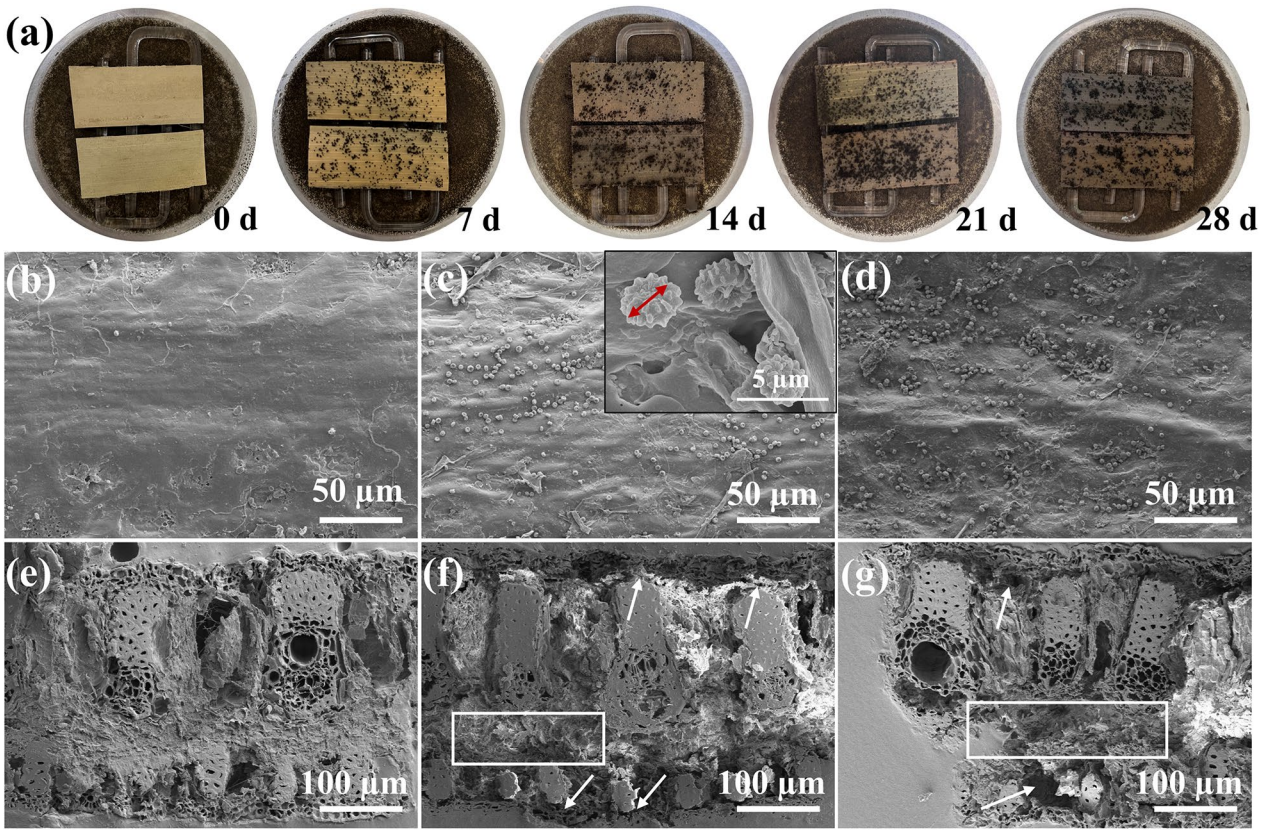

Fig. 2 Surface condition and microstructure of PLM carriers upon varying times of degradation by *A. niger*. (**a**) Surface condition, (**b**–**d**) Adaxial surface microstructural characteristics of non-degraded, 14-day, and 28-day biodegraded samples, (**e**–**g**) Cross-sectional microstructural characteristics of non-degraded, 14-day, and 28-day biodegraded samples

Chemical composition and structure

The chemical changes on the surface of PLM carriers, caused by degradation from *A. niger*, were thoroughly investigated using XPS. The dynamic evolution of the oxygen-to-carbon ratio (O/C ratio) and the C1s peak of the samples was the primary focus of the analysis. The O/C ratio is a crucial indicator for evaluating the chemical properties of the palm leaf surface, as lignin has a larger proportion of carbon atoms compared to carbohydrates [26]. As Fig. 3a illustrated, the O/C ratio on the surface of PLM carriers decreased from 0.28 to 0.17 with the increase of degradation time. This indicated a preferential depolymerization and dissolution of carbohydrates by *A. niger*, resulting in an increase of lignin content [27, 28].

Furthermore, the high-resolution XPS spectra of carbon C1s were fitted and deconvolved into four distinct sub-peaks: C1 (C-C or C-H), C2 (C-O), C3 (C=O, O-C-O), and C4 (O-C=O), as illustrated in Fig. 3b–f. Notably, the C1 peak primarily originates from lignin with phenylpropane structures, along with fatty acids, fats, waxes, and terpenoids. The C2 peak serves as a key structural indicator of cellulose and hemicellulose. The C3 peak reflects the acetal structures in hemicellulose and the carbonyl structures in lignin. Lastly, the C4 peak is closely associated with the structures of acetyl groups in hemicellulose molecules, glucuronic acid groups, resin acids and fatty acids [26, 29]. The results for the area of C 1 s peaks of PLM carriers were shown in Table 1. During the degradation process, the intensity of the C1 peak experienced a transient decrease followed by a pronounced increase. This transient decrease might be attributed to limited degradation of lipids on the surface of leaves by *A. niger*. Given its stable structure and resistance to degradation, the relative content of lignin rose significantly after 21 days of degradation by *A. niger*, leading to a corresponding rise in the intensity of the C1 peak (Fig. 3e, f). The relative content of the C2 peak initially increased and then decreased, indicating preferential degradation of the lipids on the surface of leaves. This degradation subsequently led to an increase in the relative content of holocellulose (Fig. 3b, c). *A. niger* can secrete lignocellulolytic enzymes [30]. The degradation of cellulose and hemicellulose led to a decrease in the intensity of the C2 peak after 7 days (Fig. 3d–f). In addition, the degradation of cellulose and hemicellulose generated acidic and aldehyde substances, leading to an increase in the contributions of the C3 peak before 14 days (Fig. 3d). The relative content of C4 peak decreased significantly, from 4.24 to 1.43%, further confirmed the severe degradation of hemicellulose (Fig. 3b and f).

Quantitative chemical composition studies indicate that during the degradation by *A. niger*, the hemicellulose content decreased from 22.5 to 11.2%. The extractives content first decreased from 10.6 to 8.5%, and then rose to 14.9%. Initially, the cellulose content increased from 37.5 to 39.1%, but later decreased to 33.6% (Fig. 4a). These findings suggested that under the degradation by *A. niger*, hemicellulose and lipids in the PLM carriers were preferentially degraded, followed by cellulose. The relative content of lignin increased, primarily because of its stable structure, which was more resistant to degradation. The observed increase in lignin's relative content was also a consequence of the degradation of other components.

The ATR-FTIR spectra are presented in Fig. 4b. The absorption peaks at 2917 and 2842 cm^{-1}, corresponding to asymmetric and symmetric stretching vibrations of CH_2, respectively. These peaks are closely associated with lipids in PLM carriers [10]. The reduction in the intensity of these peaks indicated that *A. niger* has the ability to degrade the lipids in the PLM carriers, which aligned with the previous XPS analysis. Furthermore, previous studies have confirmed that *A. niger* can secrete lipase to facilitate this degradation process [31]. The absorption peak at 1650 cm^{-1} corresponds to the conjugated carbonyl in lignin [32]. Notably, as *A. niger* degradation time increased, the absorption intensity of this peak remained relatively unchanged, indicating the lignin structure's high stability and resistance to degradation reactions. However, it's crucial to acknowledge the sensitivity limitations of ATR-FTIR and XPS in lignin detection, which suggested that the possibility of lignin structure modification still existed. The absorption peak near 1730 cm^{-1} is associated with the C=O stretching vibration of acetyl and carboxyl groups, serving as a crucial marker for distinguishing hemicellulose from other components including cellulose and lignin [33]. The intensity of this peak decreased significantly, confirming that hemicellulose in the PLM carrier was preferentially degraded during the early stages of fungal attack [34]. In addition, the absorption peak at 1160 cm^{-1}, attributed to the C-O-C stretching vibration in cellulose and hemicellulose, also exhibited a marked decrease in intensity during the later stages of degradation. This observation suggested that both cellulose and hemicellulose had undergone degradation at a certain degree.

Figure 5 presents the XRD diffraction patterns of the PLM carriers degraded by *A. niger*. Notably, some extra diffraction peaks of crystalline material appeared in the degraded sample compared to the control sample (Fig. 5a). This was attributed to the reaction between acidic substances secreted by *A. niger* and substances such as silica and calcium carbonate in the sample [35].

During the degradation by *A. niger*, the relative crystallinity of PLM carriers initially increased from

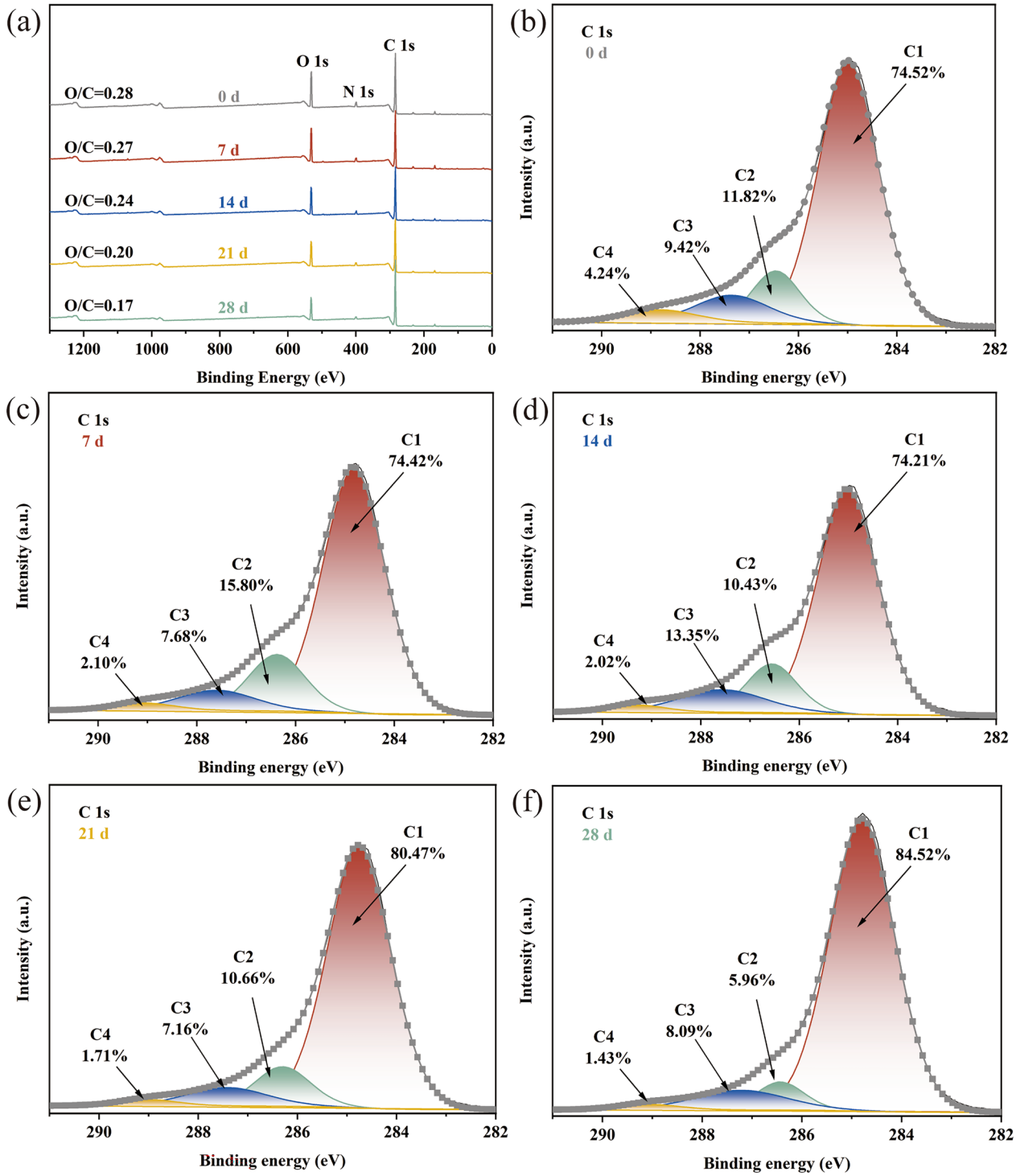

Fig. 3 XPS spectra of PLM carriers. (**a**) O/C ratio, (**b**) Non-degraded samples, (**c**) 7-day biodegraded samples, (**d**) 14-day biodegraded samples (**e**) 21-day biodegraded samples, (**f**) 28-day biodegraded samples

39.8% in the undegraded state to 56.0% after 14 days of degradation, followed by a decrease to 38.8% after 28 days (Fig. 5b). This change was due to the selective degradation of amorphous cellulose regions caused by *A. niger*, leading to an increase in the relative crystallinity of cellulose during the initial stages of degradation [36, 37].

Table 1 O/C ratio and area of C 1 s peaks of PLM carriers

Degradation time (d)	O/C ration	C1 (%)	C2 (%)	C3 (%)	C4 (%)
0	0.28	74.52	11.82	9.42	4.24
7	0.27	74.42	15.82	7.68	2.10
14	0.24	74.21	10.43	13.35	2.02
21	0.20	80.47	10.66	7.16	1.71
28	0.17	84.52	5.96	8.09	1.43

Prior research has demonstrated that a small number of unordered cellulose chains appeared on the surface of cellulose crystals, while the cellulose chains are highly ordered in the core position [38]. This structural characteristic makes crystalline cellulose resistant to microbial attack until the outer amorphous cellulose chains are fully depolymerized.

Micromechanical properties

The PLM carriers were abundant in leaf fibers, with a fiber volume fraction of approximately 23%, exhibiting a cell wall thickness of approximately 4 μm, as depicted in Fig. 6a. These fibers possess exceptional hardness properties, playing a crucial role in enhancing the mechanical strength of the PLMs. The cell walls, as the actual load-bearing unit of leaf fibers, are crucial for their mechanical performance. During the degraded period of *A. niger*,

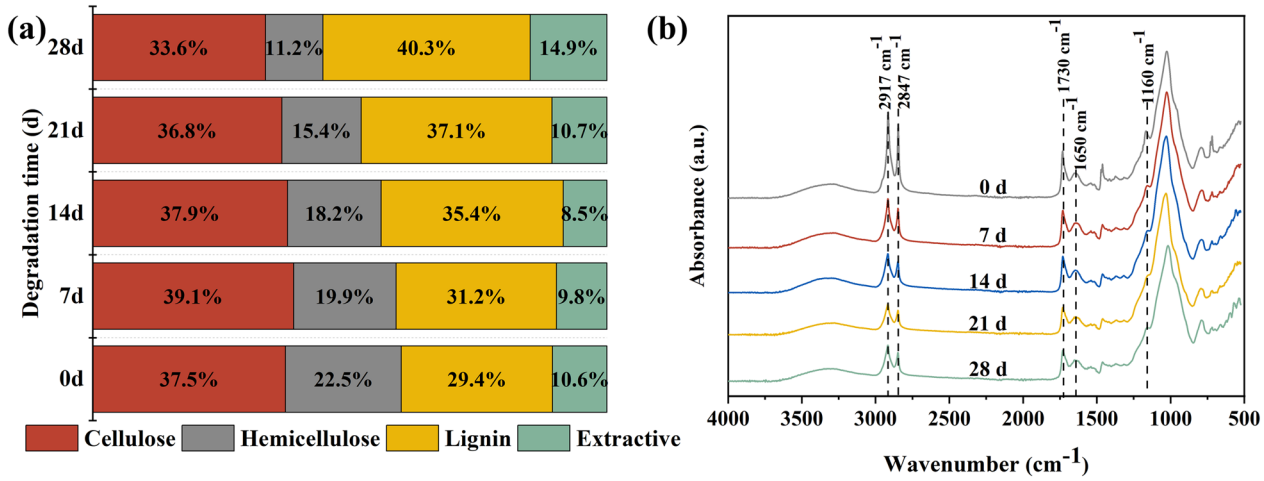

Fig. 4 (**a**) Chemical components content of PLM carriers, (**b**) ATR-FTIR spectra between 4000 and 500 cm^{-1} of PLM carriers

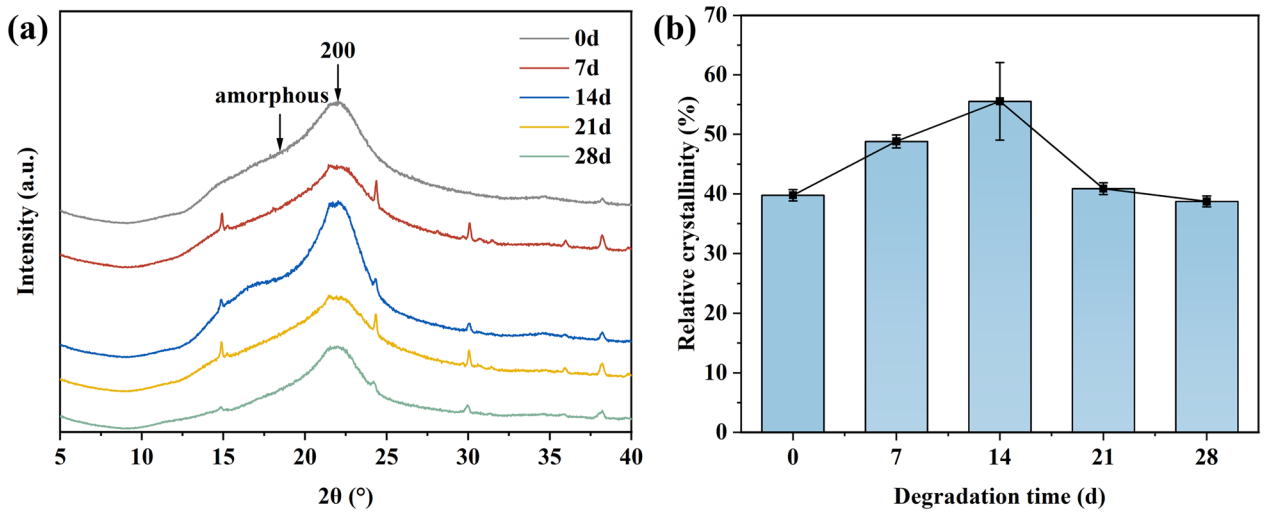

Fig. 5 Cellulose crystalline structures of PLM carriers. (**a**) X-ray diffractograms, (**b**) Relative crystallinity

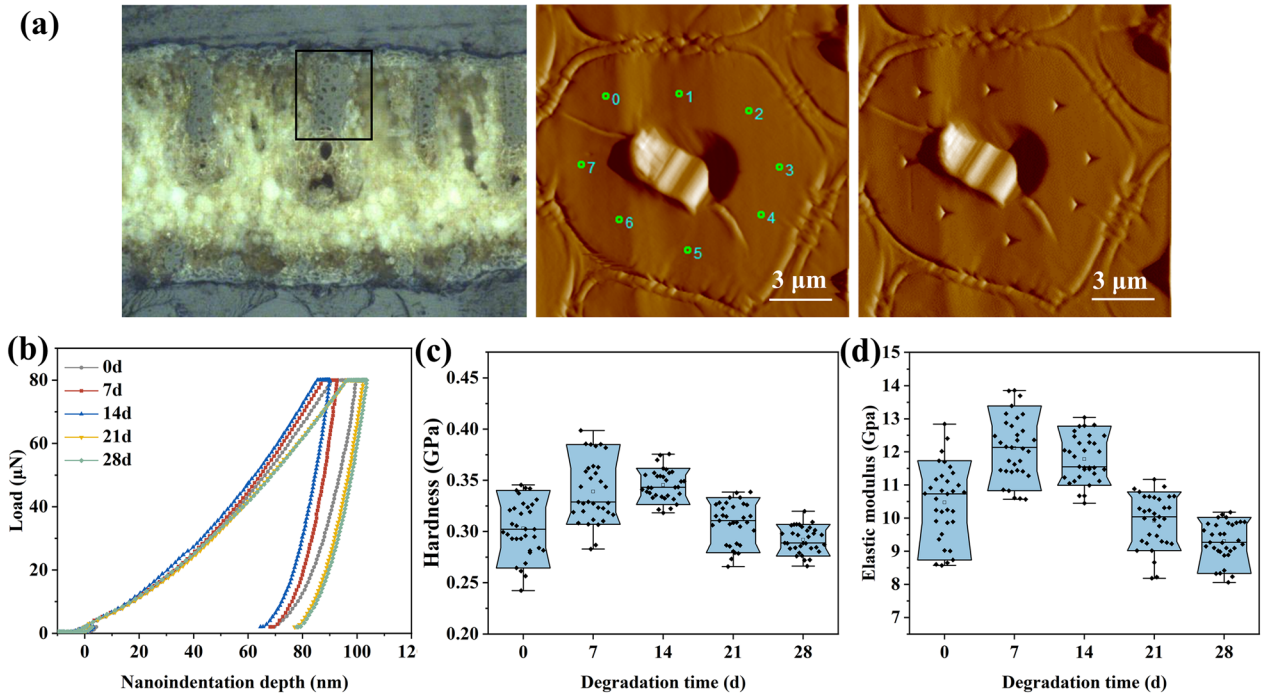

Fig. 6 Micromechanical properties of leaf fibers in PLM carriers. (**a**) Procedure of NI testing including test area, test points, and indentation after unloading, (**b**) the indentation depth-load curves, (**c**) the hardness of the leaf fiber cell walls, (**d**) the elastic modulus of the leaf fiber cell walls

changes in the chemical and crystal structure of the PLM carriers inevitably impacted the cell walls' performance. This study pioneered the utilization of nanoindentation technology to assess the micromechanical properties of PLM carriers within extremely small dimensions. This technique offered an unprecedented opportunity to delve into the micromechanical behavior of leaf fiber cell walls during mildew by *A. niger*. Furthermore, it provides a new reference for the evaluation of the deterioration degree of ancient PLMs [39].

Figure 6b depicts the indentation depth-load curves of leaf fibers from PLM carriers degraded by *A. niger* for varying durations. With increasing degradation time, the maximum indentation depth of the leaf fiber cell walls exhibited a gradual decline from 99.5 nm to 89.9 nm, followed by an increase to 103.5 nm at a force of 80 μN. Correspondingly, the hardness of the fiber cell walls increased significantly from 0.30 to 0.34 Gpa during the initial stages of mildew (Fig. 6c). In view of that the crucial role of lignin in determining cell wall hardness, this observed increase in hardness possibly resulted from the increase in lignin content resulting from the degradation of holocellulose [40]. However, a notable decrease in cell wall hardness from 0.34 GPa after degraded for 14 days to 0.29 GPa after degraded for 28 days was observed (Fig. 6c). This reduction could be attributed to lignin modification or extensive damage to hemicellulose. Similarly, the elastic modulus of cell walls also exhibited a trend of first increasing and following decreasing as the degradation time by *A. niger* increased (Fig. 6d). This trend was consistent with the changes of relative crystallinity, indicating a correlation between the elastic modulus of cell walls and the relative crystallinity of cellulose. The elastic modulus of cellulose significantly exceeds that of other chemical component, thus it could determine the elastic modulus along the longitudinal axis of the cell wall to a large extent. However, as mildew developed to later stages, the degradation of holocellulose and lignin modification resulted in the disruption of intermolecular and intramolecular bonds. This weakened the polymer connections within the leaf fiber cell walls, ultimately compromising their load-bearing capacity [41]. Consequently, there is a significant decrease in the elastic modulus of the cell walls. These findings provided important evidence for a deep understanding of the impact of mildew by *A. niger* on the performance of the PLM carriers.

Degradation mechanism analysis

The deconstruction model of *A. niger* on the PLM carriers is shown in Fig. 7. After colonizing on the PLM carriers, *A. niger* can secrete cellulose enzymes, lipases, and acidic substances, which sequentially caused progressive damage to the epidermal cells, mesophyll cells, and leaf fibers (Fig. 7a). Due to their thinner cell walls

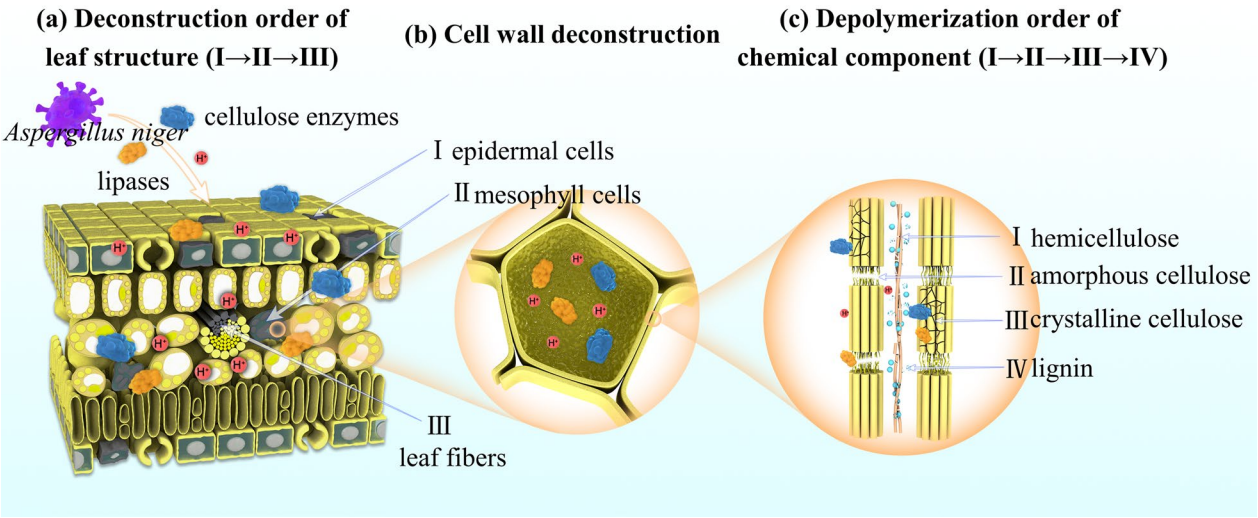

Fig. 7 The deconstruction model of *A. niger* on the PLM carriers. (**a**) Deconstruction order of leaf structure, (**b**) Cell wall deconstruction, (**c**) Depolymerization order of chemical component

and larger intercellular spaces, mesophyll cells underwent a more severe degree of degradation compared to epidermal and leaf fiber cells. Although leaf fibers were the primary contributors to the stiffness and strength of the leaf, effectively enhancing the stability of the leaf structure, the severe degradation of mesophyll cells led to the destruction of the interfaces between different tissue structures within the leaf. This led to the separation of different tissue structures, negatively impacting the physical properties of the PLMs, and consequently causing macroscopic manifestations such as peeling and fiber warping on the surfaces of PLMs. Moreover, lipases can degrade lipid substances and wax on the leaf surface, facilitating *A. niger* to degrade the interior part of leaves. Cellulose enzymes and acidic substances can successively depolymerize hemicellulose, amorphous cellulose, and crystalline cellulose (Fig. 7c). The degradation of hemicellulose and amorphous cellulose resulted in an increase of the relative crystallinity of cellulose, thereby enhancing the hardness and elastic modulus of the leaf fiber cell walls. However, upon further degradation of crystalline cellulose, the hardness and elastic modulus of the leaf fiber cell walls decreased significantly. Simultaneously, the disruption of intermolecular and intramolecular bonds of holocellulose caused severe brittleness in the PLMs. This fragile state induced the ink and color on the ancient PLMs to fade and fall off more easily. This degradation model of *A. niger* on the PLM carriers provides important scientific guidance for further studying the degradation evolution mechanism and protection strategies of *A. niger* on wooden cultural relics.

Conclusion

The ancient PLMs preserved in the Dai Autonomous Prefecture of Xishuangbanna, Yunnan, China, have been colonized by *A. niger* fungus. In order to gain a comprehensive understanding of the fungal impact on the PLM carriers, the *A. niger* was employed to degrade the carriers in this study. Subsequently, a systematic investigation was conducted to assess the microscopic morphology, chemical composition, crystal structure, and micromechanical properties of the degraded PLMs. During the degradation process, *A. niger* secreted cellulose enzymes, lipases, and acidic substances, gradually destroying the epidermal cells, mesophyll cells, and leaf fibers of the PLM carriers. Lipid substances and wax on the surface of carriers were first degraded, followed by the sequential depolymerization of hemicellulose, amorphous cellulose, and crystalline cellulose. Lignin was resistant to degradation due to its stable structure. Additionally, the hardness and elastic modulus of the leaf fiber cell walls exhibited a trend of first increasing and following decreasing, closely related to factors such as the chemical composition and crystal structure of the cell walls. This study provides a comprehensive understanding of the deterioration and evolution process of hierarchical structures within PLM carriers under *A. niger* degradation. Additionally, it is firstly to employ nanoindentation technology in examining the micromechanical properties of PLMs. These findings serve as a scientific basis for assessing the extent of PLM deterioration and provide valuable references for the preservation of organic cultural relics, including PLMs and wooden artifacts.

Abbreviations

PLM	Palm leaf manuscript
NI	Nanoindentation
SEM	Scanning electron microscopy
XPS	X-ray photoelectron spectroscopy
ATR-FTIR	Attenuated total reflectance-Fourier transform infrared spectrometry
XRD	X-ray diffraction
PDA	Potato Dextrose Agar
DNA	Deoxyribonucleic acid
PCR	Polymerase chain reaction

Supplementary Information

The online version contains supplementary material available at https://doi.org/10.1186/s40494-024-01320-3.

Supplementary Material 1.

Acknowledgements
The authors express their gratitude to Liusan Li, Li Li, Xiangdong Li, and Bingfeng Zhang for their assistance with this study.

Author contributions
The manuscript was prepared through contributions of all authors. SC carried out the experiments, conducted all data analysis, and wrote most of the manuscript. LL and XT provided experimental samples, defined the research project, and designed the experiments. All authors have given approval to the final version of the manuscript.

Funding
This work was supported by the National Key Research and Development Program of China (No.2022YFF0903903).

Availability of data and materials
All data generated or analyzed during this study are included in this published article.

Declarations

Ethics approval and consent to participate
This article does not contain any data based on experiments in humans or animals.

Consent for publication
Not applicable.

Competing interests
The authors declare no competing interests.

Received: 13 March 2024 Accepted: 7 June 2024
Published online: 17 June 2024

References

1. Sah A. Palm leaf manuscripts of the world: material, technology and conservation. Stud Conserv. 2002;47(1):15–24. https://doi.org/10.1179/sic.2002.47.Supplement-1.15.
2. Wiland J, Brown R, Fuller L, Havelock L, Johnson J, Kenn D, Kralka P, Muzart M, Pollard J, Snowdon J. A literature review of palm leaf manuscript conservation—part 1: a historic overview, leaf preparation, materials and media, palm leaf manuscripts at the British Library and the common types of damage. J Inst Conserv. 2022;45(3):236–59. https://doi.org/10.1080/19455224.2022.2115093.
3. Wang Y, Wen M, Zhou X, Gao F, Tian S, Jue D, Lu H, Zhang Z. Automatic damage identification of Sanskrit palm leaf manuscripts with SegFormer. Herit Sci. 2024;12(1):8. https://doi.org/10.1186/s40494-023-01125-w.
4. Crowley AS. Repair and conservation of palm-leaf manuscripts. Restaurator. 1970;1:105–14. https://doi.org/10.1515/rest.1970.1.2.105.
5. Lian X, Yu C, Han W, Li B, Zhang M, Wang Y, Li L. Revealing the mechanism of ink flaking from surfaces of palm leaves (*Corypha umbraculifera*). Langmuir. 2024;40(12):6375–83. https://doi.org/10.1021/acs.langmuir.3c03946.
6. Wiland J, Brown R, Fuller L, Havelock L, Johnson J, Kenn D, Kralka P, Muzart M, Pollard J, Snowdon J. A literature review of palm leaf manuscript conservation—part 2: historic and current conservation treatments, boxing and storage, religious and ethical issues, recommendations for best practice. J Inst Conserv. 2023;46(1):64–91. https://doi.org/10.1080/19455224.2023.2167095.
7. Alexander TJ, Kumar SS. A novel binarization technique based on whale optimization algorithm for better restoration of palm leaf manuscript. J Amb Intel Hum Comp. 2020. https://doi.org/10.1007/s12652-020-02546-2.
8. Zhang M, Song X, Wang J, Lyu X. Preservation characteristics and restoration core technology of palm leaf manuscripts in Potala Palace. Arch Sci-Netherlands. 2022;22(4):501–19. https://doi.org/10.1007/s10502-021-09383-y.
9. Zhang M, Song X, Wang Y. Two different storage environments for palm leaf manuscripts: comparison of deterioration phenomena. Restaurator. 2021;42(3):147–68. https://doi.org/10.1515/res-2021-0003.
10. Chu S, Lin L, Tian X. Evaluation of the deterioration state of historical palm leaf manuscripts from Burma. Forests. 2023;14(9):1775. https://doi.org/10.3390/f14091775.
11. Cavalli A, Cibecchini D, Togni M, Sousa HS. A review on the mechanical properties of aged wood and salvaged timber. Constr Build Mater. 2016;114:681–7. https://doi.org/10.1016/j.conbuildmat.2016.04.001.
12. Suryawanshi D, Sinha P, Agrawal O. Basic studies on the properties of palm leaf. Restaurator. 1994;15:65–78. https://doi.org/10.1515/rest.1994.15.2.65.
13. Singh AP, Kim YS, Chavan RR. Advances in understanding microbial deterioration of buried and waterlogged archaeological woods: a review. Forests. 2022;13(3):394. https://doi.org/10.3390/f13030394.
14. Castillo-Hernández D, Sánchez-Ramírez F, Jiménez-Pérez JL, Cruz-Orea A, Correa-Pacheco ZN. Study of ancient paper and detection of microbiological contamination using photoacoustic technique. Int J Thermophys. 2020;41(36):1–14. https://doi.org/10.1007/s10765-020-2612-3.
15. Rakotonirainy M, Lavédrine B. Screening for antifungal activity of essential oils and related compounds to control the biocontamination in libraries and archives storage areas. Int Biodeterior Biodegrad. 2005;55(2):141–7. https://doi.org/10.1016/j.ibiod.2004.10.002.
16. Geweely N, Abu Taleb A, Ibrahim S, Grenni P, Caneva G, Galotta G, Abdallah M, Atwa D, Plaisier J, Antonelli F. New data on relevant ancient Egyptian wooden artifacts: identification of wooden species and study of the state of conservation with multidisciplinary analyses. Archaeometry. 2023;65(1):165–83. https://doi.org/10.1111/arcm.12815.
17. Fierascu I, Fierascu R, Stirban A, Panaitescu D, Nicolae C, Raditoiu V, Zgarciu M, Leahu A. Chemical and mineral characterization of Romanian book paper materials (XVII–XIXth century). Microchem J. 2020;152:104307. https://doi.org/10.1016/j.microc.2019.104307.
18. Cao J, Liu X, Wan J, Chen H, Liu D, Li J, Mai B. Analysis of microbial diversity and its degradation function in wooden piles at Shahe ancient bridge site in Xi'an and protection measures. Herit Sci. 2024;12:33. https://doi.org/10.1186/s40494-024-01157-w.
19. Liu S, Ran Y, Cao J. Comparison on thermally modified beech wood in different mediums: morphology, chemical change and water-related properties. Ind Crops Prod. 2024;209:117935. https://doi.org/10.1016/j.indcrop.2023.117935.
20. Sluiter A, Hames B, Ruiz R, Scarlata C, Sluiter J, Templeton D, Crocker D. Determination of structural carbohydrates and lignin in biomass. Lab Anal Proced. 2008;1617(1):1–16.
21. Segal L, Greely JJ, Martin AE, Conrad CM. An empirical method for estimating the degree of crystallinity of native cellulose using the X-ray diffractometer. Text Res J. 1959;29(10):786–94. https://doi.org/10.1177/004051755902901003.
22. Oliver WC, Pharr GM. An improved technique for determining hardness and elastic modulus using load and displacement sensing indentation

experiments. J Mater Res. 1992;7(6):1564–83. https://doi.org/10.1557/JMR.1992.1564.
23. El-Dawy E, Hussein M, El-Nahas S. Description and management of *Aspergillus* section *Nigri* causing post-harvest bulbs rot of onion. Sci Rep. 2024;14:6076. https://doi.org/10.1038/s41598-024-53849-9.
24. Area MC, Cheradame H. Paper aging and degradation: recent findings and research methods. BioResources. 2011;6(4):5307–37. https://doi.org/10.1537/biores.6.4.5307-5337.
25. Fouda A, Abdel-Nasser M, Khalil AMA, Hassan SE-D, Abdel-Maksoud G. Investigate the role of fungal communities associated with a historical manuscript from the 17th century in biodegradation. Npj Mat Degrad. 2022;6(1):88. https://doi.org/10.1038/s41529-022-00296-4.
26. Kocaefe D, Huang X, Kocaefe Y, Boluk Y. Quantitative characterization of chemical degradation of heat-treated wood surfaces during artificial weathering using XPS. Surf Interface Anal. 2012;45(2):639–49. https://doi.org/10.1002/sia.5104.
27. Inari GN, Petrissans M, Lambert J, Ehrhardt JJ, Gérardin P. XPS characterization of wood chemical composition after heat-treatment. Surf Interface Anal. 2006;38(10):1336–42. https://doi.org/10.1002/sia.2455.
28. Xing X, Li S, Jin J, Lin L, Zhou Y, Peng L, Fu F. Effect of high-intensity microwave (HIMW) treatment on chemistry of radiata pine. Wood Sci Technol. 2023;57(5):1077–97. https://doi.org/10.1007/s00226-023-01487-1.
29. Wang W, Zhu Y, Cao J, Sun W. Correlation between dynamic wetting behavior and chemical components of thermally modified wood. Appl Surf Sci. 2015;324:332–8. https://doi.org/10.1016/j.apsusc.2014.10.139.
30. Cardoso Duarte J, Costa-Ferreira M. *Aspergilli* and lignocellulosics: enzymology and biotechnological applications. Fems Microbiol Rev. 1994;13(2–3):377–86. https://doi.org/10.1111/j.1574-6976.1994.tb00057.x.
31. Alabdalall AH, Alanazi NA, Aldakeel SA, AbdulAzeez S, Borgio JF. Molecular, physiological, and biochemical characterization of extracellular lipase production by *Aspergillus niger* using submerged fermentation. Peerj. 2020;8:e9425. https://doi.org/10.7717/peerj.9425.
32. Traore M, Kaal J, Martinez CA. Application of FTIR spectroscopy to the characterization of archeological wood. Spectrochim Acta A. 2016;153:63–70. https://doi.org/10.1016/j.saa.2015.07.108.
33. Fang S, Lyu X, Tong T, Lim AI, Li T, Bao J, Hu YH. Turning dead leaves into an active multifunctional material as evaporator, photocatalyst, and bioplastic. Nat Commun. 2023;14(1):1203. https://doi.org/10.1038/s41467-023-36783-8.
34. Khaliliyan H, Lin J, Jusner P, Schiehser S, Bacher M, Kostić M, Rosenau T, Potthast A, Böhmdorfer S. Profiling of historical rag papers by their non-cellulosic polysaccharide composition. Carbohyd Polym. 2024;326:121611. https://doi.org/10.1016/j.carbpol.2023.121611.
35. Füchtner S, Alfredsen G, Thygesen LG. Oxalate found in wood cell wall during incipient brown rot degradation. Int Biodeter Biodegr. 2023;177:105531. https://doi.org/10.1016/j.ibiod.2022.105531.
36. Zhu Y, Li W, Meng D, Li X, Goodell B. Non-enzymatic modification of the crystalline structure and chemistry of Masson pine in brown-rot decay. Carbohydr Polym. 2022;286:119242. https://doi.org/10.1016/j.carbpol.2022.119242.
37. Guo J, Chen J, Meng Q, Ploszczanski L, Ja Liu, Luo R, Jin T, Siedlaczek P, Lichtenegger HC, Yin Y, Rennhofer H. Molecular and crystal structures of cellulose in severely deteriorated archaeological wood. Cellulose. 2022;29(18):9549–68. https://doi.org/10.1007/s10570-022-04856-4.
38. Tai H, Chang C, Cai W, Lin J, Huang S, Lin Q, Yuan E, Li S, Lin Y, Chan JCC, Tsao C. Wood cellulose microfibrils have a 24-chain core-shell nanostructure in seed plants. Nat Plants. 2023;9(7):1154–68. https://doi.org/10.1038/s41477-023-01430-z.
39. Faisal NH, Ahmed R, Goel S, Cross G. Future of nanoindentation in archaeometry. J Mater Res. 2018;33(17):2515–32. https://doi.org/10.1557/jmr.2018.280.
40. Wang Z, Xu E, Fu F, Lin L, Yi S. Characterization of wood cell walls treated by high-intensity microwaves: effects on physicochemical structures and micromechanical properties. Ind Crop Prod. 2022;187:115341. https://doi.org/10.1016/j.indcrop.2022.115341.
41. Chu S, Lin L, Zhang Y, Wang D. Physicochemical structure and micromechanical properties of archaeological wood under alternating dry and wet conditions. Wood Mater Sci Eng. 2023. https://doi.org/10.1080/17480272.2023.2286628.

Publisher's Note